Arbitrary direction incident Gaussian beam scattering by multispheres*

Li Zheng-Jun(李正军), Wu Zhen-Sen(吴振森)†,
Li Huan(李 焕), and Li Hai-Ying(李海英)

School of Science, Xidian University, Xi'an 710071, China

(Received 28 June 2010; revised manuscript received 23 February 2011)

Based on spherical vector wave functions and their coordinate rotation theory, the field of a Gaussian beam in terms of the spherical vector wave functions in an arbitrary unparallel Cartesian coordinate system is expanded. The beam shape coefficient and its convergence property are discussed in detail. Scattering of an arbitrary direction Gaussian beam by multiple homogeneous isotropic spheres is investigated. The effects of beam waist width, sphere separation distance, sphere number, beam centre positioning, and incident angle for a Gaussian beam with two polarization modes incident on various shaped sphere clusters are numerically studied. Moreover, the scattering characteristics of two kinds of shaped red blood cells illuminated by an arbitrary direction incident Gaussian beam with two polarization modes are investigated. Our results are expected to provide useful insights into particle sizing and the measurement of the scattering characteristics of blood corpuscle particles with laser diagnostic techniques.

Keywords: multiple scattering, Gaussian beam, biological particle

PACS: 11.80.La, 13.88.+e, 52.25.Os, 34.80.Qb **DOI:** 10.1088/1674-1056/20/8/081101

1. Introduction

Calculations on the light-scattering properties of plane waves or laser beams from an aggregate of particles are used in many areas, such as biophysics, microbiology, medicine, oceanography, meteorological optics, and so on. Since the advent of the classic Mie theory,[1] many investigators[2−9] have studied the scattering properties of spherical particles. The addition theorem of spherical vector wave functions (SVWFs) was put forward in Ref. [10] and developed in Refs. [2], [3], and [5], and the first significant contribution to multisphere scattering through the provision of a comprehensive solution for a two-sphere chain was made in Ref. [2]. Then, the scattering of an aggregate of spherical particles in a general case is solved based on the generation multiple Mie theory (GMM) developed by Xu,[4,6−8] T-matrix approach developed by Wang and Chew[11] and Auger *et al.*,[12] and discrete-dipole approximation (DDA) developed by Bruce and Flatau[13] and Lei *et al.*[14] However, these approaches are limited to the plane wave scattering problem. If a Gaussian beam is used as an excitation source and the beam waist width is less than or of the same order as the sphere separation distance of two adjacent spheres, the plane wave assumption utilized in these earlier analyses will not be valid.

The problem of a Gaussian beam scattering by multispheres has not yet been figured out, while a Gaussian beam is a typical laser beam and used extensively in particle sizing, laser fusion, optical levitation, laser beam cloud penetration, etc.[15] Gerard *et al.*[16] derived three methods to compute the beam shape coefficient (BSC) g_n (on-axis) and g_n^m (off-axis) based on several relatively simple approximate Gaussian beam models introduced by Davis[17] and put forward the generalized Lorenz–Mie theory (GLMT) to solve the problem of a Gaussian beam scattering by multispheres.[18] Utilizing the addition theorem of the SVWFs, Doicu and Wriedt[19] presented the BSC of the off-axis Gaussian beam through different methods. Wu *et al.*[20] also put forward an improved algorithm of BSC. Subsequently, many authors have further studied various cases of a particle scattering Gaussian beam.[15,21−23] However, most of the above references dealt only with a single object scattering the Gaussian beam. Due to the difficulty and complexity of the BSC calculation and the addition theorem co-

*Project supported by the Fundamental Research Funds for the Central Universities of China and National Natural Science Foundation of China (Grant No. 60771038).

†Corresponding author. E-mail: wuzhs@mail.xidian.edu.cn

© 2011 Chinese Physical Society and IOP Publishing Ltd

efficients used to solve the interaction of two spheres in the multi-particle scattering problem, published results on multiple scattering Gaussian beam are rather scarce. Based on the "order-of-scattering" technique introduced by Fuller and Kattawar,[9] Barton *et al.*[24] investigated the internal field and far-region scattering field of only two adjacent spheres scattering a focused Gaussian beam. Bai *et al.*[25] investigated the interaction of a sphere chain with a Gaussian beam. However, in their study, the incident direction of the Gaussian beam and the direction of the sphere chain were completely coincident, as a result, they adopted the BSC and the addition theorem coefficients in the simplest case, namely, the on-axis BSC and the addition theorem coefficients while $m = \pm 1$. In the present paper, a more complicated scattering problem where arbitrarily distributed aggregate spheres scatter an off-axis Gaussian beam is studied. The off-axis BSC and the addition theorem coefficients while $m = -n$, n are considered.

In some particle sizing experimentations, the laboratory coordinate system is fixed. Hence, it is necessary to change the incident direction of the Gaussian beam to obtain more scattering information about fixed aggregate particles. However, the BSC in the laboratory coordinate system is difficult to derive. In this paper, BSC in arbitrary unparallel Cartesian coordinate system is derived through the introduction of Euler angles α, β, γ[26] and the coordinate-rotation theory of the SVWF in two unparallel Cartesian coordinate systems.[27] The BSC is more complicated than the off-axis BSC and its convergence property is numerically discussed. Afterwards, the analytical solution on the multisphere particles with arbitrary configuration scattering an arbitrary direction incident Gaussian beam is derived based on the GMM developed in Refs. [4], [6]–[8]. Some selected figures on the total scattering intensities of various shaped sphere clusters and red blood cells (RBCs) illuminated by x'-polarization or y'-polarization Gaussian beams with different beam waist widths and different incident angles are presented. This work is helpful for providing some theoretical tools and benchmarks for further research on the transfer and scattering of a Gaussian beam by an aggregate of particles which are randomly distributed. In the subsequent depiction, a time dependence of the form $\exp(-\mathrm{i}\omega t)$ is assumed and suppressed, where ω is the circular frequency.

2. Theoretical formulation

2.1. BSC in arbitrary coordinate system

In order to indicate the randomicity of the incident direction of Gaussian beam and the configuration of the aggregation of spherical particles, a Cartesian coordinate system $Oxyz$ is built and serves as a fixed global coordinate system. As shown in Fig. 1, L homogeneous isotropic spheres with radii a_j $(j = 1, 2, \ldots, L)$ in $Oxyz$ are illuminated by a z'-propagating monochromatic Gaussian beam polarized in $x'O'z'$-plane, which is characterized by the transverse component of the electric field in the beam coordinate system $O'x'y'z'$ as

$$E_{\mathrm{i}x}(x'', y'', 0) = E_0 \exp[-(x''^2 + y''^2)/w_0^2], \qquad (1)$$

where E_0 is the amplitude of the beam centre O', w_0 is the beam waist width and the y'-axis component $E_{\mathrm{i}y}(x'', y'', 0) = 0$.

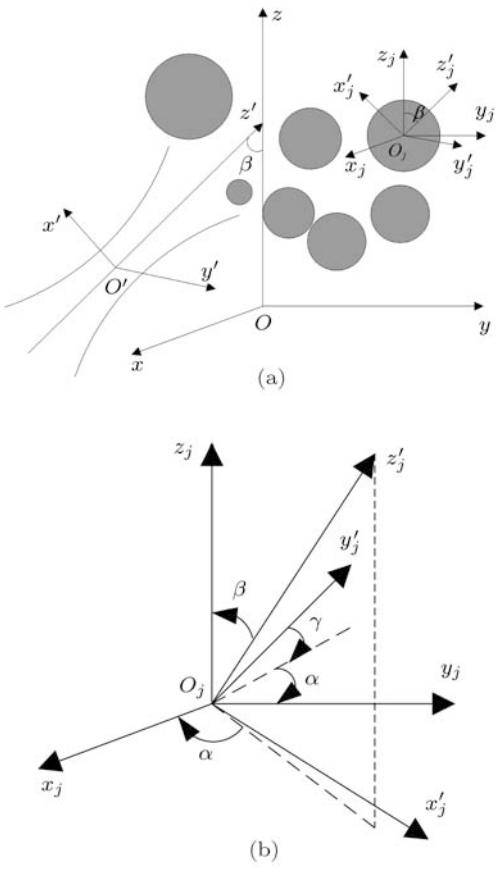


Fig. 1. L spheres illuminated by an arbitrary direction incident Gaussian beam.

We establish a rectangular coordinate system $O_j x_j y_j z_j$ with an arbitrary sphere centre O_j, which is parallel to $Oxyz$. Due to the randomicity of the

incident direction, $O_jx_jy_jz_j$ and $O'x'y'z'$ are not always parallel. Accordingly, the field of the incident Gaussian beam cannot be simply expanded in terms of the SVWF's in the j-th sphere coordinate system $O_jx_jy_jz_j$. Thus, a temporary coordinate system $O_jx'_jy'_jz'_j$ parallel to $O'x'y'z'$ is introduced to make the field of the incident Gaussian beam be expanded in terms of the SVWF in $O_jx'_jy'_jz'_j$ as

$$\begin{aligned}\boldsymbol{E}_{ij'}(\boldsymbol{r}) &= E_0\sum_{n=1}^{\infty}\sum_{m=-n}^{n}C_{nm}[\mathrm{i}g_{n,\mathrm{TE}}^{mj'}\boldsymbol{M}_{mn}^{(1)} \\ &\quad + g_{n,\mathrm{TM}}^{mj'}\boldsymbol{N}_{mn}^{(1)}], \\ \boldsymbol{H}_{ij'}(\boldsymbol{r}) &= E_0\frac{k_0}{\omega\mu_0}\sum_{n=1}^{\infty}\sum_{m=-n}^{n}C_{nm}[g_{n,\mathrm{TE}}^{mj'}\boldsymbol{N}_{mn}^{(1)} \\ &\quad - \mathrm{i}g_{n,\mathrm{TM}}^{mj'}\boldsymbol{M}_{mn}^{(1)}], \end{aligned} \tag{2}$$

where

$$C_{nm} = \begin{cases} \mathrm{i}^{n-1}\dfrac{2n+1}{n(n+1)}, & m \geq 0, \\ (-1)^{|m|}\dfrac{(n+|m|)!}{(n-|m|)!}\mathrm{i}^{n-1}\dfrac{2n+1}{n(n+1)}, & m < 0. \end{cases} \tag{3}$$

The SVWF $\boldsymbol{M}$ and $\boldsymbol{N}$ can be written as[1,4]

$$\begin{aligned}&\boldsymbol{M}_{mn}^{(l)}(kr,\theta,\phi) \\ &= \mathrm{z}_n^{(l)}(kr)\left[\mathrm{i}m\frac{\mathrm{P}_n^m(\cos\theta)}{\sin\theta}\,\mathrm{e}^{\mathrm{i}m\phi}\hat{\theta} - \frac{\mathrm{d}\mathrm{P}_n^m(\cos\theta}{\mathrm{d}\theta}\,\mathrm{e}^{\mathrm{i}m\phi}\hat{\phi}\right], \\ &\boldsymbol{N}_{mn}^{(l)}(kr,\theta,\phi) \\ &= n(n+1)\frac{z_n^{(l)}(kr)}{kr}\mathrm{P}_n^m(\cos\theta)\,\mathrm{e}^{\mathrm{i}m\phi}\hat{r} + \frac{1}{kr}\frac{\mathrm{d}(rz_n^{(l)}(kr))}{\mathrm{d}r} \\ &\quad\times\left[\frac{\mathrm{d}\mathrm{P}_n^m(\cos\theta)}{\mathrm{d}\theta}\hat{\theta} + \mathrm{i}m\frac{\mathrm{P}_n^m(\cos\theta)}{\sin\theta}\hat{\phi}\right]\mathrm{e}^{\mathrm{i}m\phi}, \end{aligned} \tag{4}$$

where $\mathrm{z}_n^{(l)}$ represents an appropriate kind of spherical Bessel functions: the first kind j_n, the second kind y_n, or the third kind $\mathrm{h}_n^{(1)}$ and $\mathrm{h}_n^{(2)}$, denoted by $l = 1, 2, 3$, or 4, respectively; $\mathrm{P}_n^m(\cos\theta)$ is the associated Legendre function of the first kind.

The expansion coefficients $g_{n,\mathrm{TE}}^{mj'}$ and $g_{n,\mathrm{TM}}^{mj'}$ in Eq. (2) are the so-called BSCs. The field of the Gaussian beam is not a rigorous solution to the vector wave equation, so it is difficult to give an analytical form of the BSC. However, various approximate solutions have been given, as discussed in the introduction. The Gaussian beam arbitrarily polarized in $x'O'z'$-plane can be decomposed into two orthogonally linear polarization beams, namely, an x'-polarization beam and a y'-polarization beam. If there are no particular requirements for accuracy and beam waist width, the localized approximation with the sum of series, given by Doicu and Wriedt,[19] is a preferable selection, owing to the calculation time. For the x'-polarization Gaussian beam, the BSC can be expressed as

$$\begin{aligned}\begin{bmatrix} g_{n,\mathrm{TM}}^{mj'} \\ \mathrm{i}g_{n,\mathrm{TE}}^{mj'} \end{bmatrix} &= (-1)^{m-1}K_{nm}\psi'_j\,\mathrm{e}^{\mathrm{i}k_0z'_j} \\ &\quad\times\frac{1}{2}\left[\mathrm{e}^{\mathrm{i}(m-1)\varphi'_j}J_{m-1}\left(2\frac{\bar{Q}'_j\rho'_j\rho_n}{w_0^2}\right)\right. \\ &\quad\left.\pm\,\mathrm{e}^{\mathrm{i}(m+1)\varphi'_j}J_{m+1}\left(2\frac{\bar{Q}'_j\rho'_j\rho_n}{w_0^2}\right)\right], \end{aligned} \tag{5}$$

where

$$\begin{aligned}\psi'_j &= \mathrm{i}\bar{Q}'_j\exp(-\mathrm{i}\bar{Q}'_j\rho_j^{'2}/w_0^2) \\ &\quad\times\exp(-\mathrm{i}\bar{Q}'_j(n+0.5)^2/k_0^2w_0^2), \\ \bar{Q}'_j &= (\mathrm{i}-2z'_j/(k_0w_0^2))^{-1}, \\ \rho'_j &= \sqrt{x_j^{'2}+y_j^{'2}},\quad \rho_n = (n+0.5)/k_0, \\ \varphi'_j &= \arctan(x'_j/y'_j),\quad k_0 = 2\pi/\lambda, \end{aligned} \tag{6}$$

$$K_{nm} = \begin{cases} (-\mathrm{i})^{|m|}\dfrac{\mathrm{i}}{(n+0.5)^{|m|-1}}, & m \neq 0, \\ \dfrac{n(n+1)}{n+0.5}, & m = 0, \end{cases} \tag{7}$$

where $(x'_j,\ y'_j,\ z'_j)$ is the coordinate of the beam centre O' in the temporary coordinate system $O_jx'_jy'_jz'_j$. The subscript or superscript $j = 1, 2, \ldots, L$ indicates the relative parameter of the j-th sphere. In what follows, the formulae are shown to have similar expressions in the two coordinate systems.

For arbitrary two coordinate systems with the same origin such as the temporary coordinate system $O_jx'_jy'_jz'_j$ and the j-th coordinate system $O_jx_jy_jz_j$ shown in Fig. 1, the rotation relations of these coordinate systems can be described by the Euler angles α, β, γ.[26] Generally, the coordinates of the beam centre O' and the j-th sphere centre in global coordinate system $Oxyz$ are known and assumed to be $(x',\ y',\ z')$ and $(x_j,\ y_j,\ z_j)$, respectively. Accordingly, the coordinate $(x'_j,\ y'_j,\ z'_j)$ can be obtained through the coordinate rotation theory to be

$$\begin{aligned}\begin{pmatrix} x'_j \\ y'_j \\ z'_j \end{pmatrix} &= \begin{pmatrix} \cos\alpha & -\sin\alpha & 0 \\ \sin\alpha & \cos\alpha & 0 \\ 0 & 0 & 1 \end{pmatrix}\begin{pmatrix} \cos\beta & 0 & -\sin\beta \\ 0 & 1 & 0 \\ \sin\beta & 0 & \cos\beta \end{pmatrix} \\ &\quad\times\begin{pmatrix} \cos\gamma & -\sin\gamma & 0 \\ \sin\gamma & \cos\gamma & 0 \\ 0 & 0 & 1 \end{pmatrix}\begin{pmatrix} x'-x_j \\ y'-y_j \\ z'-z_j \end{pmatrix}. \end{aligned} \tag{8}$$

The BSC in the temporary coordinate system $O_jx'_jy'_jz'_j$ parallel to the beam coordinate system

$O'x'y'z'$ has now been obtained, but what we want is the BSC in the j-th coordinate system $O_jx_jy_jz_j$. For $O_jx'_jy'_jz'_j$ and $O_jx_jy_jz_j$, the SVWFs in these coordinate systems have the following relation with Euler angles α, β and γ[27]

$$(\boldsymbol{M},\boldsymbol{N})^{(1)}_{mn}(kr'_j,\theta'_j,\varphi'_j) = \sum_{s=-n}^{n}\rho\,(m,s,n)(\boldsymbol{M},\boldsymbol{N})^{(1)}_{sn}\,(kr_j,\theta_j,\varphi_j)\,, \quad (9)$$

where

$$\rho(m,s,n) = (-1)^{s+m}\,\mathrm{e}^{\mathrm{i}s\gamma}\left[\frac{(n+m)!(n-s)!}{(n-m)!(n+s)!}\right]^{1/2} \times u^{(n)}_{sm}(\beta)\,\mathrm{e}^{\mathrm{i}m\alpha}, \quad (10)$$

with

$$u^{(n)}_{sm}(\beta) = \left[\frac{(n+s)!(n-s)!}{(n+m)!(n-m)!}\right]^{1/2} \times\sum_{\sigma}\binom{n+m}{n-s-\sigma}\binom{n-m}{\sigma}(-1)^{n-s-\sigma} \times\left(\cos\frac{\beta}{2}\right)^{2\sigma+s+m}\left(\sin\frac{\beta}{2}\right)^{2n-2\sigma-s-m}. \quad (11)$$

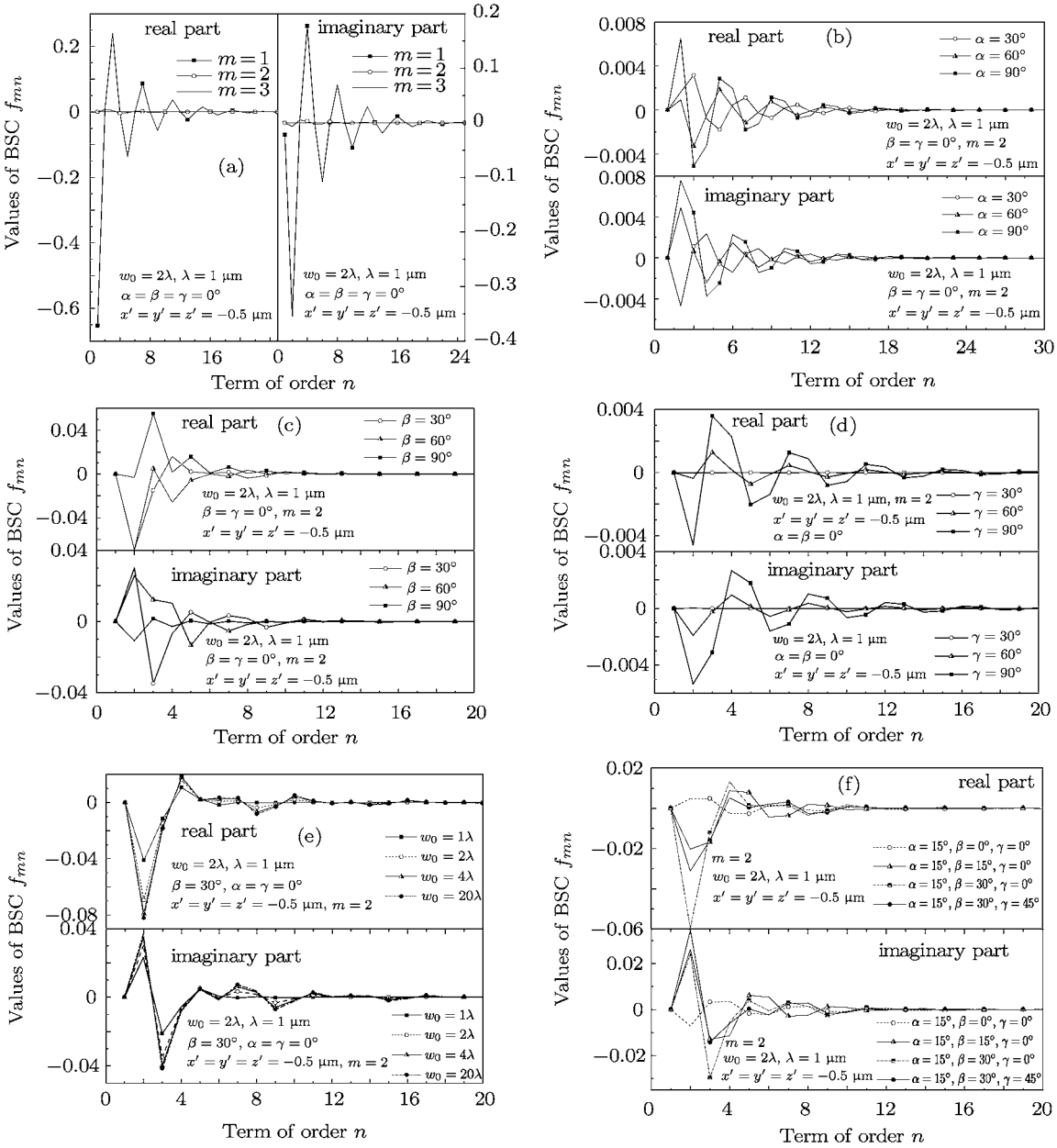


Fig. 2. Values of BSC f_{mn} versus term of order n.

Substituting Eq. (9) into Eq. (2) and interchanging between summation orders, m and s, the expansion of the field of the incident Gaussian beam in terms of the SVWF in arbitrary j-th sphere coordinate system can be derived as

$$\boldsymbol{E}_{ij} = -E_0 \sum_{n=1}^{\infty} \sum_{m=-n}^{n} \left[f_{mn}^{ij} \boldsymbol{N}_{mn}^{(1)} - \mathrm{i} g_{mn}^{ij} \boldsymbol{M}_{mn}^{(1)} \right],$$

$$\boldsymbol{H}_{ij} = E_0 \frac{k_0}{\omega \mu_0} \sum_{n=1}^{\infty} \sum_{m=-n}^{n} \left[g_{mn}^{ij} \boldsymbol{N}_{mn}^{(1)} + \mathrm{i} f_{mn}^{ij} \boldsymbol{M}_{mn}^{(1)} \right], \quad (12)$$

where f_{mn}^{ij} and g_{mn}^{ij} are the BSC in the arbitrary j-th sphere coordinate system and can be expressed as

$$\left(f_{mn}^{ij}, -g_{mn}^{ij}\right) = \sum_{s=-n}^{n} \rho(s,m,n) C_{ns} \times \left(g_{n,\mathrm{TM}}^{sj'}, g_{n,\mathrm{TE}}^{sj'}\right), \quad (13)$$

and $\rho(s,m,n)$ can be obtained through interchanging between m and s in Eq. (12). For the y'-polarization Gaussian beam, we can also obtain the BSC through similar derivation as

$$\left(f_{mny'}^{ij}, g_{mny'}^{ij}\right) = -\mathrm{i}\left(f_{mn}^{ij}, -g_{mn}^{ij}\right), \quad (14)$$

In as much as the simple relation, we only need to study the characteristic of either BCS. Some selected results are given in order to study the property of the BCS for an x'-polarization Gaussian beam as follows.

Figure 2 shows the values of BSC f_{mn} versus the term of the order n in several cases. It can be observed that (i) the BSC has an excellent convergence property with the increase of the term of the order n in each case shown above; (ii) the larger the term of the order m, the quicker the convergence is (see Fig. 2(a); (iii) Euler angles α, β and γ have little influence on convergence speed, but strongly affect the magnitude of the BSC as compared with Figs. 2(b)–2(d) and 2(f); (iv) the larger the beam waist width, the slower the convergence is and the larger the magnitude of the BSC is (see Fig. 2(e)).

2.2. Scattered and internal fields of each sphere

The scattered and internal fields can be expanded in terms of the SVWFs in the j-th sphere coordinate system $O_j x_j y_j z_j$,

$$\boldsymbol{E}_{sj} = E_0 \sum_{n=1}^{\infty} \sum_{m=-n}^{n} \left[a_{mn}^{sj} \boldsymbol{N}_{mn}^{(3)} - \mathrm{i} b_{mn}^{sj} \boldsymbol{M}_{mn}^{(3)} \right],$$

$$\boldsymbol{H}_{sj} = -E_0 \frac{k_0}{\omega \mu_0} \sum_{n=1}^{\infty} \sum_{m=-n}^{n} \times \left[b_{mn}^{sj} \boldsymbol{N}_{mn}^{(3)} + \mathrm{i} a_{mn}^{sj} \boldsymbol{M}_{mn}^{(3)} \right], \quad (15)$$

$$\boldsymbol{E}_{Ij} = -E_0 \sum_{n=1}^{\infty} \sum_{m=-n}^{n} \left[A_{mn}^{Ij} \boldsymbol{N}_{mn}^{(1)} - \mathrm{i} B_{mn}^{Ij} \boldsymbol{M}_{mn}^{(1)} \right],$$

$$\boldsymbol{H}_{Ij} = E_0 \frac{k_j}{\omega \mu_j} \sum_{n=1}^{\infty} \sum_{m=-n}^{n} \times \left[B_{mn}^{Ij} \boldsymbol{N}_{mn}^{(1)} + \mathrm{i} A_{mn}^{Ij} \boldsymbol{M}_{mn}^{(1)} \right], \quad (16)$$

where $k_j = 2\pi N_j/\lambda$, μ_0 and μ_j are the permeability of the free space and the j-th dielectric sphere, respectively.

2.3. Total incident fields of each sphere

The interaction between two arbitrary spheres should be considered for multi-particle scattering problem, resulting in the fact that the total incident fields of each sphere consists of not only the initial incident field but also the scattered fields from the other spheres. For instance, the total incident fields on the j-th sphere should be expressed as

$$\boldsymbol{E}_{itj} = \boldsymbol{E}_{ij} + \sum_{(l \neq j)}^{L} \boldsymbol{E}_{sl,j},$$

$$\boldsymbol{H}_{itj} = \boldsymbol{H}_{ij} + \sum_{(l \neq j)}^{L} \boldsymbol{H}_{sl,j}, \quad (17)$$

where $l = 1, 2, \ldots, L$ and $j = 1, 2, \ldots, L$. In order to predigest the forms of the total incident fields, we need to use the addition theorem of the SVWF. For any two parallel coordinate systems, the addition theorem is actually to seek the relations of the SVWF between these two coordinate systems. As shown in Fig. 3, for arbitrary two parallel coordinate systems $O_l x_l y_l z_l$ and $O_j x_j y_j z_j$, the SVWF in these coordinate systems have the following relations[2,5,10]

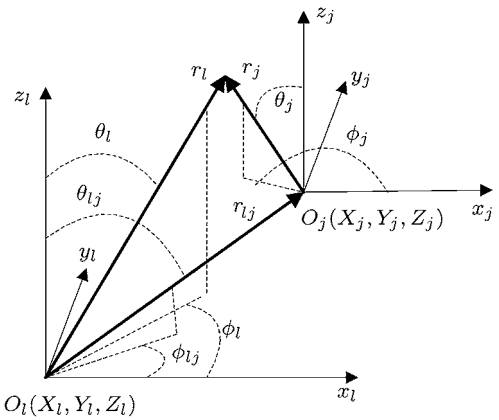


Fig. 3. Transform of coordinate system for addition theorem.

when $r_l \leq d_{lj}, r_l \leq d_{lj}$,

$$\begin{cases} \boldsymbol{M}_{mn}^{(3)}(r_l,\theta_l,\phi_l) = \sum\limits_{v=1}^{\infty}\sum\limits_{\mu=-v}^{v}[A_{\mu v}^{mn}(l,j)\boldsymbol{M}_{\mu v}^{(1)}(r_j,\theta_j,\phi_j) + B_{\mu v}^{mn}(l,j)\boldsymbol{N}_{\mu v}^{(1)}(r_j,\theta_j,\phi_j)], \\ \boldsymbol{N}_{mn}^{(3)}(r_l,\theta_l,\phi_l) = \sum\limits_{v=1}^{\infty}\sum\limits_{\mu=-v}^{v}[A_{\mu v}^{mn}(l,j)\boldsymbol{N}_{\mu v}^{(1)}(r_j,\theta_j,\phi_j) + B_{\mu v}^{mn}(l,j)\boldsymbol{M}_{\mu v}^{(1)}(r_j,\theta_j,\phi_j)]; \end{cases} \tag{18}$$

when $r_l \geq d_{lj}, r_j \geq d_{lj}$,

$$\begin{cases} \boldsymbol{M}_{mn}^{(3)}(r_l,\theta_l,\phi_l) = \sum\limits_{v=1}^{\infty}\sum\limits_{\mu=-v}^{v}[\tilde{A}_{\mu v}^{mn}(l,j)\boldsymbol{M}_{\mu v}^{(3)}(r_j,\theta_j,\phi_j) + \tilde{B}_{\mu v}^{mn}(l,j)\boldsymbol{N}_{\mu v}^{(3)}(r_j,\theta_j,\phi_j)], \\ \boldsymbol{N}_{mn}^{(3)}(r_l,\theta_l,\phi_l) = \sum\limits_{v=1}^{\infty}\sum\limits_{\mu=-v}^{v}[\tilde{A}_{\mu v}^{mn}(l,j)\boldsymbol{N}_{\mu v}^{(3)}(r_j,\theta_j,\phi_j) + \tilde{B}_{\mu v}^{mn}(l,j)\boldsymbol{M}_{\mu v}^{(3)}(r_j,\theta_j,\phi_j)], \end{cases} \tag{19}$$

where A and B are addition theorem coefficients and the detailed expressions can be obtained from Refs. [2], [4] and [5]. Then, substituting Eqs. (18), (12), and (15) into Eq. (17), we can derive the total incident fields of each sphere as

$$\begin{aligned} \boldsymbol{E}_{itj} &= E_0\sum_{n=1}^{\infty}\sum_{m=-n}^{n}[\,f_{mn}^{itj}\boldsymbol{N}_{mn}^{(1)}(k_0r_j,\theta_j,\phi_j) \\ &\quad - \mathrm{i}g_{mn}^{itj}\boldsymbol{M}_{mn}^{(1)}(k_0r_j,\theta_j,\phi_j)], \\ \boldsymbol{H}_{itj} &= -E_0\frac{k_0}{\omega\mu_0}\sum_{n=1}^{\infty}\sum_{m=-n}^{n}[\,g_{mn}^{itj}\boldsymbol{N}_{mn}^{(1)}(k_0r_j,\theta_j,\phi_j) \\ &\quad + \mathrm{i}f_{mn}^{itj}\boldsymbol{M}_{mn}^{(1)}(k_0r_j,\theta_j,\phi_j)], \end{aligned} \tag{20}$$

where

$$\begin{aligned} f_{mn}^{itj} &= -f_{mn}^{ij} + \sum_{(l\neq j)}^{L}\sum_{v=1}^{\infty}\sum_{\mu=-v}^{v}[a_{\mu v}^{sl}A_{mn}^{\mu v}(l,j) \\ &\quad - \mathrm{i}b_{\mu v}^{sl}B_{mn}^{\mu v}(l,j)], \quad (l\neq j), \\ g_{mn}^{itj} &= -g_{mn}^{ij} + \sum_{(l\neq j)}^{L}\sum_{v=1}^{\infty}\sum_{\mu=-v}^{v}[\mathrm{i}a_{\mu\nu}^{sl}B_{mn}^{\mu v}(l,j) \\ &\quad + b_{\mu v}^{sl}A_{mn}^{\mu v}(l,j)], \quad (l\neq j). \end{aligned} \tag{21}$$

2.4. Scattering coefficients

For the j-th sphere, the boundary conditions are written as

$$\begin{aligned} &E_{it\theta j} + E_{s\theta j} = E_{I\theta j}, \\ &E_{it\phi j} + E_{s\phi j} = E_{I\phi j}, \quad (r_j = a_j), \\ &H_{it\theta j} + H_{s\theta j} = H_{I\theta j}, \\ &H_{it\phi j} + H_{s\phi j} = H_{I\phi j}, \quad (r_j = a_j). \end{aligned} \tag{22}$$

Utilizing the expressions of the SVWFs (4), the components of the total incident fields, the scattered and internal fields can be gained and substituting them into Eq. (22), as done in Mie theory,[1] the interactive scattering coefficients can be derived easily as

$$a_{mn}^{sj} = a_n^j f_{mn}^{itj}, \quad b_{mn}^{sj} = b_n^j g_{mn}^{itj}, \tag{23}$$

where a_n^j and b_n^j are Mie scattering coefficients.[1] The total scattered fields are our concerned problem and can be written as

$$\boldsymbol{E}_{st} = \sum_{l=1}^{L}\boldsymbol{E}_{sl}, \quad \boldsymbol{H}_{st} = \sum_{l=1}^{L}\boldsymbol{H}_{sl}. \tag{24}$$

Using the addition theorem (19), the total scattered fields of the entire aggregation in the global coordinate system can be obtained as

$$\begin{aligned} \boldsymbol{E}_{st} &= E_0\sum_{n=1}^{\infty}\sum_{m=-n}^{n}\left[a_{mn}^{st}\boldsymbol{N}_{mn}^{(3)} - \mathrm{i}b_{mn}^{st}\boldsymbol{M}_{mn}^{(3)}\right], \\ \boldsymbol{H}_{st} &= \frac{-E_0k_0}{\omega\mu_0}\sum_{n=1}^{\infty}\sum_{m=-n}^{n}\left[b_{mn}^{st}\boldsymbol{N}_{mn}^{(3)} + \mathrm{i}a_{mn}^{st}\boldsymbol{M}_{mn}^{(3)}\right], \end{aligned} \tag{25}$$

where

$$\begin{aligned} a_{mn}^{st} &= a_{mn}^{sj_0} + \sum_{l\neq j_0}^{L}\sum_{v=1}^{\infty}\sum_{\mu=-v}^{v}[a_{\mu v}^{s2}\tilde{A}_{mn}^{\mu v}(l,j_0) \\ &\quad - \mathrm{i}b_{mn}^{s2}\tilde{B}_{mn}^{\mu v}(l,j_0)], \\ b_{mn}^{st} &= b_{mn}^{sj_0} + \sum_{l\neq j_0}^{L}\sum_{v=1}^{\infty}\sum_{\mu=-v}^{v}[\mathrm{i}a_{\mu v}^{s2}\tilde{B}_{mn}^{\mu v}(l,j_0) \\ &\quad + b_{mn}^{s2}\tilde{A}_{mn}^{\mu v}(l,j_0)]. \end{aligned} \tag{26}$$

For the y'-polarization Gaussian beam, the scattering coefficients can be similarly obtained by using Eq. (4) in the above derivation.

Substituting Eq. (4) into Eq. (25), we can derive the normalized total far-region scattering intensity for scattering electric field as

$$\begin{aligned} I_{st} &= I_{s\parallel} + I_{s\perp} \\ &= \lim_{r->\infty} k^2r^2\{|E_{st\theta}|^2 + |E_{st\phi}|^2\}/|E_0|^2, \\ &= \frac{1}{\pi}\Big\{\Big|\sum_{n=1}^{\infty}\sum_{m=-n}^{n}(-\mathrm{i})^n\,\mathrm{e}^{\mathrm{i}m\phi} \end{aligned}$$

$$\times [a_{mn}^{st}\tau_{mn} - \mathrm{i}b_{mn}^{st}m\pi_{mn}]\Big|^2 + \Big|\sum_{n=1}^{\infty}\sum_{m=-n}^{n}(-\mathrm{i})^{n+1}\,\mathrm{e}^{\mathrm{i}m\phi} \times [-a_{mn}^{st}m\pi_{mn} + \mathrm{i}b_{mn}^{st}\tau_{mn}]\Big|^2\Big\}, \quad (27)$$

where $I_{s\parallel}$ and $I_{s\perp}$ denote the scattering intensities in the directions parallel and perpendicular to the scattering plane, respectively.

3. Results and discussion

In this section, we focus mainly on the effects of the beam waist width, sphere separation distance, sphere number, beam center positioning, polarization and incident angle for a Gaussian beam incidence. Moreover, the most general theory is used to study the scattering characteristic of biological particles. The total scattering intensity of various shaped RBCs illuminated by an arbitrary direction incident Gaussian beam with x'-axis or y'-axis polarization is presented.

3.1. Validation of theory and codes

To validate the theory, some results are selected to be compared with the published data and numerical results provided by the CST software. As shown in Fig. 4(a), the total scattering intensities of closely packed pyramid-like aggregate acrylic spheres illuminated by a z-propagating Gaussian beam with $w_0 = 20\lambda$ and two polarization modes are compared with those obtained from the program "gmm01f.f" which is provided and applied to the GMM by Xu,[4,6–8] and the CST software for a plane wave incidence, respectively. The good agreement can confirm the accuracy of our theory and the dependability of the CST software.

Like Fig. 4(a), figure 4(b) shows the angular distributions, but the incident angle $\beta = 30°$ and beam waist width $w_0 = 1\lambda$, 2λ, 3λ, and 20λ. It is observed for either polarization mode that i) the total scattering intensity increases with the increase of the beam waist width for an oblique incident Gaussian beam, while a similar performance for a normally incident Gaussian beam on a sphere chain has been studied by Bai;[25] ii) both the curves "$w_0 = 20\lambda(x'\text{-P})$" and "$w_0 = 20\lambda(y'\text{-P})$" are in good agreement with the corresponding curves "CST" offered by the CST software, which can testify the correctness of our theory formulae for the arbitrary incident direction Gaussian beam scattered further; and iii) the peak values and their oscillation positioning of the curves for x'-P and y'-P are distinct except for the maxima at the incident direction.

It is worthwhile noting that "x'-P" and "y'-P" denote "x'-polarization" and "y'-polarization", respectively; the observing plane azimuth angle is 0° in Fig. 4, namely, xoz plane. The following figures also have the same expressions. The incident angle $\alpha = 0°$ and $\gamma = 0°$ in Fig. 4, which indicates that xoz plane and the $x'oz'$ plane are consistent and the y axis of the global coordinate system $Oxyz$ and y' axis of the beam coordinate system $O'x'y'z'$ are the same. It can be observed from Fig. 1(b).

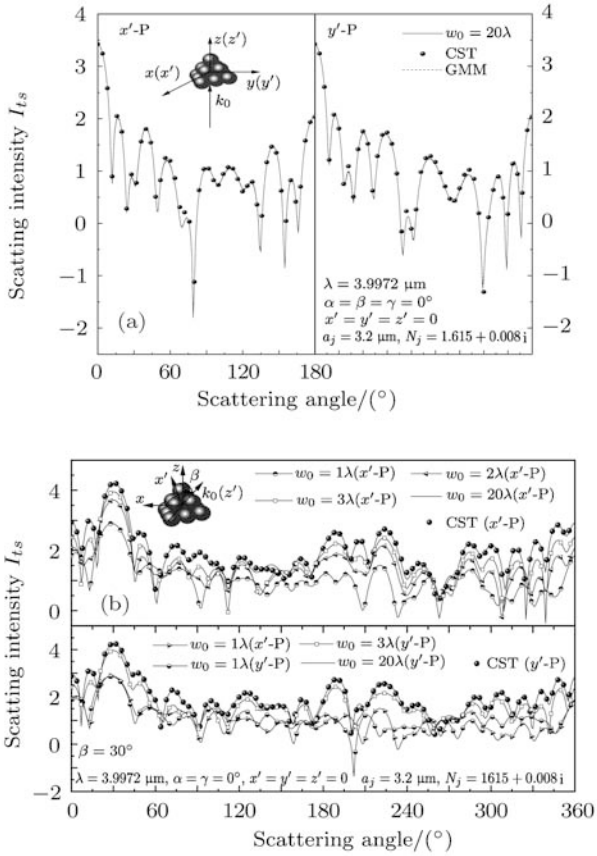


Fig. 4. Angular distributions of scattering intensity of 14 acrylic spheres for (a) positive incidence and (b) oblique incidence.

3.2. Effects of sphere separation distance and sphere number

Angular distributions of the total scattering intensity of 3-close-packed-water-drop chain illuminated by a vertical incident Gaussian beam with different waist widths are shown in Fig. 5(a). It can be found that 1) the lager the beam waist width, the higher the oscillation of the angular distribution is and the closer

to the incident direction (90°) the first extremum point resulting from the fact that as the beam waist width increases, the interaction among the contiguous spheres is more obvious, the interference point will be moved and produced; 2) the angular distribution, when the beam waist width is very small comparing with the radius, approaches that of a sphere, which indicates that the interaction is quite weak. This property can be applied to the study of particle sizing. Figure 5(b) shows the angular distributions for two polarization modes. It can be observed that the oscillation of the angular distribution for x'-P is shaper than that for y'-P at the backward direction (270°) and lateral direction (0°), owing to the stronger interaction for x'-P. Comparing Fig. 5(b) with Fig. 4(b), we find that the range of the same scattering intensity of a sphere chain is larger than that of a pyramid-like aggregate spheres at forward direction for both x'-P and y'-P due to better symmetry of a sphere chain. Furthermore, the angular distribution is symmetrical with respect to the incident axis as a result of the symmetries of both the sphere chain and the Gaussian beam.

Like Fig. 5, figure 6 shows the angular distributions for different values of sphere separation distance d_j, different sphere numbers, different incident angles and beam centres. In view of the symmetry, angular distributions only from 90° to 270° are shown in Fig. 6(a). It can be observed from Fig. 6(a) that (I) the larger the sphere separation distance d_j, the more the angular distribution coincides with that of a sphere and the smaller the oscillation period of the scattering intensity in the lateral direction (150°–230°). This is because as d_j increases, the interaction among the adjacent spheres weakens and the interaction will be existent until $d_j \geq 100a_j$. This observation might be very useful in particle sizing with laser diagnostic techniques; (II) the sphere number only affects the scattering intensity in the lateral direction (150°–230°) and the larger the sphere number, the stronger the interaction in the lateral direction (150°–230°) is, then the more the extremum points to the lateral direction (150°–230°). In Fig. 6(b), the scattering intensities

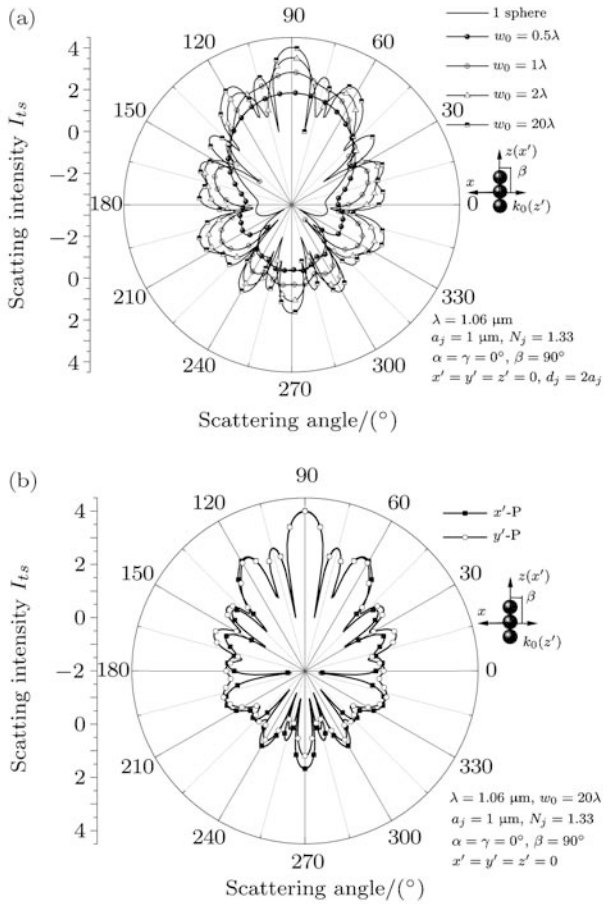


Fig. 5. Angular distributions of scattering intensity of a sphere chain consisting of 3 water drops. (a) Different beam waist widths. (b) Different polarization modes.

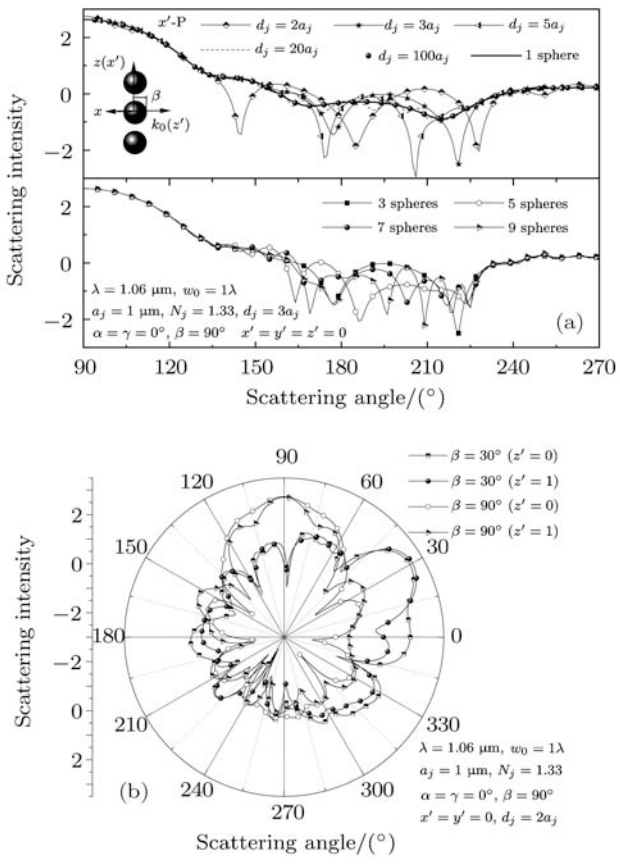


Fig. 6. Angular distributions of the scattering intensity of different sphere chains consisting of 3 water drops. (a) Different sphere separation distances and sphere number, and (b) different incident angles and beam centre positioning.

for incident angle $\beta = 30°$ and $90°$ and beam centre position $z' = 0$ and 1 μm are described, respectively. It can be observed that the symmetry of the distribution of the scattering intensity is destroyed completely when the symmetry axis of the Gaussian beam is not coincident with that of the aggregate spheres.

3.3. Effects of beam centre positioning

Angular distributions of the total scattering intensity of a closely packed tetrahedral cluster illuminated by an x'-P or a y'-P Gaussian beam with the beam centre moving away from the centre of the cluster along the z axis and the x axis are described in Fig. 7. It can be indicated that I) for both x'-P and y'-P Gaussian beams, as the beam centre moves away from the centre of the cluster along the z axis or the x axis, the scattering intensity always decreases as a result of the incident beam spreading, however, the angular distribution little changes; II) the velocity of the reduction of the scattering intensity when beam is incident along the x axis is much larger than that along the z axis as a result of the incident beam off z axis.

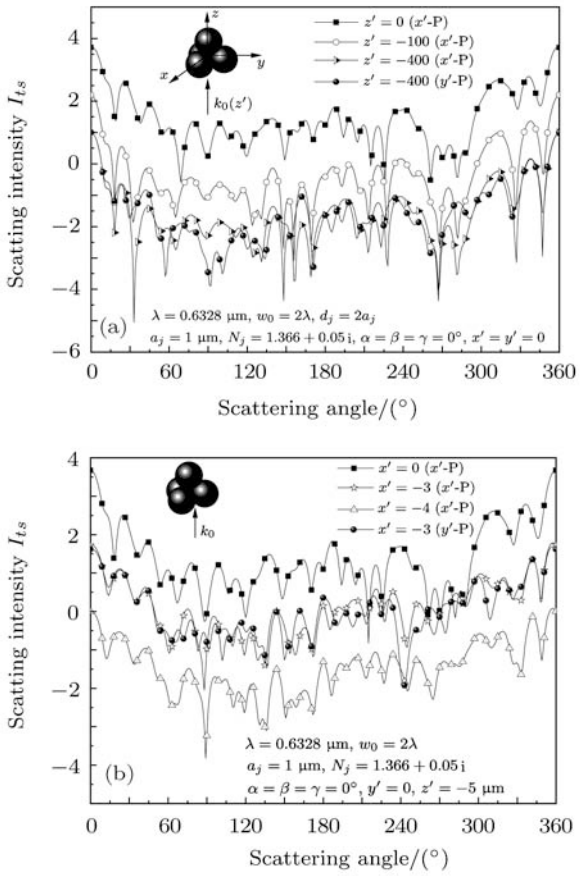


Fig. 7. Angular distributions of scattering intensity of a closely packed tetrahedral cluster. (a) Away from the centre along z axis and (b) away from the centre along x axis.

After careful examinations and simulations, it is found that the scattering intensity has a similar scattering performance for beam centre moving away from the centre of the cluster along the y axis to that along the x axis. Hence, the figures of the angular distributions of the total scattering intensity for beam centre moving away from the centre of the cluster along the y axis are not given here in detail due to the paper length restriction.

By comparing Fig. 7(a) with Fig. 7(b), it can be found that the scattering intensities at 0°–10° for x'-P and y'-P Gaussian beams propagating along the z axis are the same because the symmetry axis of the Gaussian beam is coincident with the z axis. When the Gaussian beam propagates off z axis, the scattering intensity for x'-P Gaussian beam is totally different because the symmetry axis of the Gaussian beam is not coincident with the z axis.

3.4. Scattering characteristics of biological particles

A red blood cell (RBC) is a classic biological particle. Owing to blood plasma proteins and under sufficiently low flow rates, erythrocytes fasten together along their axis of symmetry and form aggregates called rouleaux.[28] Thus, the RBC can be approximated as a blood swatch of a spherical particle cluster. Generally, the RBC in blood is characterized by radius $a = 3.5$ μm and refractive index $N = 1.47$ and the refractive index of the blood swatch is often assumed to be 1.3325–1.360. Here we adopt 1.34. Later, we will exhibit some selected angular distributions of the total scattering intensity of some shaped cluster composed of a few RBCs illuminated by a Gaussian beam with different incident angles and beam waist widths.

Figure 8(a) shows the angular distributions of the total scattering intensity of a closely packed sphere chain composed of 3 RBCs illuminated by an x'-P Gaussian beam with different beam waist widths. It can be found that a) the scattering intensity at the incident direction is not the maximal value when the beam waist width ($w_0 = 1\lambda$) is smaller than the radius of the RBC since the interaction magnitude of two adjacent RBCs is comparable to the scattering intensity of an RBC, then the effect of the interaction will be obvious. When w_0 is comparable to the radius of the RBC, the effect of the interaction in a forward direction will be very weak; b) the oscillation of the scattering intensity of 3 RBCs is sharper than that of an RBC, which is also due to the effect of the inter-

action. As Fig. 8(a), figure 8(b) shows angular distributions for the Gaussian beam with different incident angles. It can be observed that the forward scattering intensities are different for different incident angles as a result of interaction or interference magnitude in the incident direction for different incident angles. By comparing Fig. 5 with Fig. 8, it can be found that the angular distribution of the scattering intensity of the RBCs oscillates more sharply than that of the water drops because of the larger size parameter of the RBC than that of the water drop.

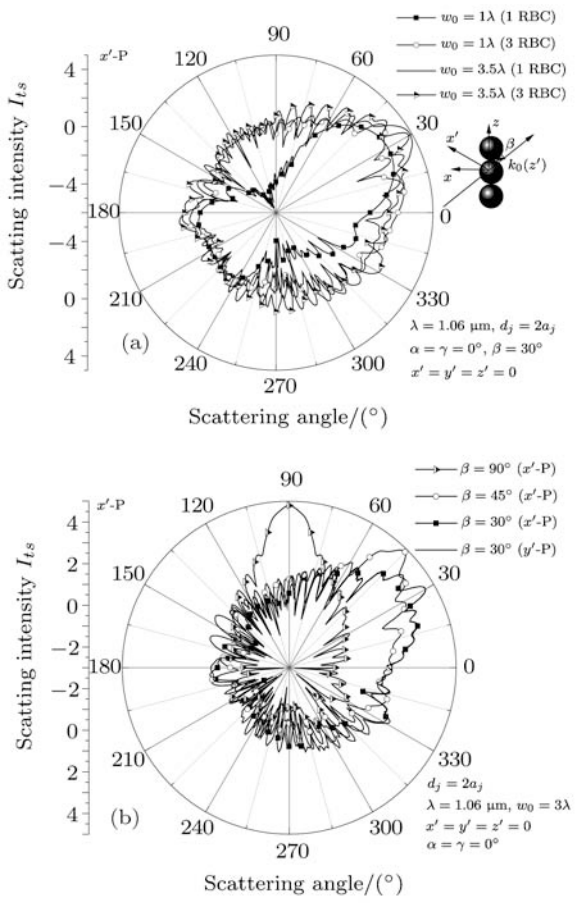


Fig. 8. Angular distributions of scattering intensity of a closely packed sphere chain composed of 3 RBCs: (a) different beam waist widths and (b) different incident angles.

Figure 9 shows angular distributions of the total scattering intensity of a trigonal cluster symmetrical along the x axis, composed of 3 RBCs illuminated by an x'-P or y'-P Gaussian beam with different values of incident angle α, β and γ. It can be observed that the forward scattering intensities of a closely packed trigonal cluster composed of 3 RBCs also change with incident angle. A comparison among Figs. 9(a), 8(b), 7, 5(b), and 4(b) indicates that the scattering intensities of x'-P and y'-P Gaussian beams are affected by the configuration of the aggregate sphere, the incident direction and the beam centre positioning of the Gaussian beam.

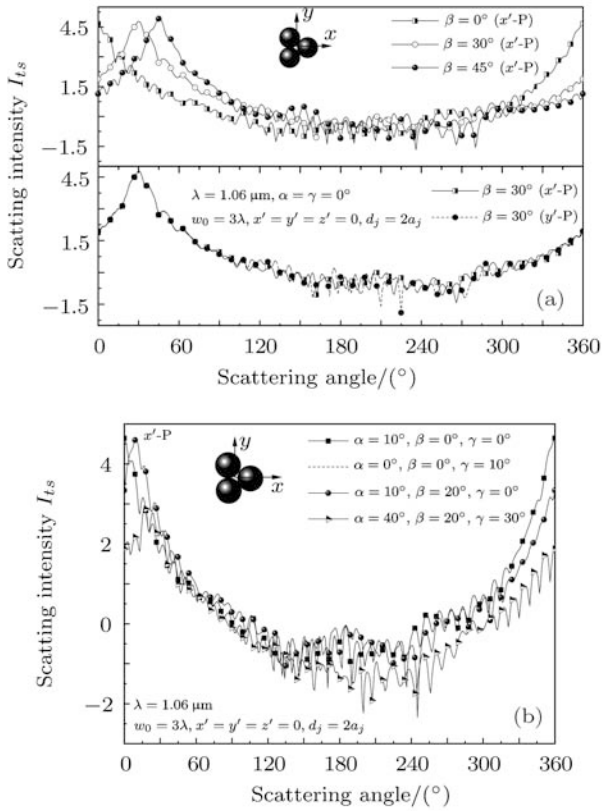


Fig. 9. Angular distributions of scattering intensity of a closely packed trigonal cluster composed of 3 RBCs; (a) changing incident angle β and (b) changing incident angle α, β and γ.

For arbitrary incident angle α, β, and γ, while $\beta = 0°$, changing α or γ by the same magnitude, we will obtain absolute scattering intensity. This can be explained through Fig. 1 as follows: while $\beta = 0°$, the incident direction of the Gaussian beam keeps unchanged if we change α or γ by the same magnitude. When $\alpha = 0°$, the position of the forward scattering intensity is determined by β. In fact, Euler angles α and β, scattering angle θ and azimuth angle φ are related as $\alpha = \varphi$ and $\beta = \theta$. When $\alpha = 0°$, different α values only denote different observing planes correspondingly. When α, β and γ are all not equal to 0°, the scattering intensity will be quite sensitive to the Euler angles.

4. Conclusion

The BSC in an arbitrary unparallel Cartesian coordinate system is derived based on the coordinate

rotation theory of the SVWF. The convergence property of the BSC for the terms of orders n and m, the incident angle and the beam waist width are numerically discussed. In addition, the most general case for an aggregate of spheres scattering an arbitrary direction incident Gaussian beam with two polarization modes is studied based on the GMM. The accuracy of the theory is verified by comparing the numerical results, while the Gaussian beam degenerates as a plane wave incidence, with the results obtained from the published data and CST software, separately. The effects of the beam parameters and the sphere separation distance on scattering property are numerically analysed. It is indicated that the beam waist width and the beam centre position moving away from the cluster centre along the x axis and the z axis have little influence on angular distribution, but they affect the magnitude of the scattering intensity significantly. The angular distribution of the total scattering intensity is determined just by the sphere illuminated by the Gaussian beam, when the sphere separation is very large or the beam waist width is very small compared with the sphere radius. The scattering properties and the polarization characteristics of various shaped clusters composed of RBCs illuminated by a Gaussian beam with different incident angles and beam waist widths are also discussed in detail.

It is worthwhile to note that the theory and the numerical arithmetic described in this paper are applicable to the randomly distributed aggregated spherical particles whose radii are comparable to the incident wavelength, including aggregation particles statistically distributed in spatial coordinate such as soot aggregation particles. We can study its scattering characteristic using this theory through simulating its spatial configuration using the Monte Carlo method. In addition, the theoretical method and the numerical results in this paper are conducible to an effective calibration for further research on the transfers and scattering of the Gaussian beam on randomly distributed particles, to the study of particle sizing with laser diagnostic techniques and the reverse scattering problem for aggregation particles.

Acknowledgment

The authors are greatly grateful to Yu-Lin Xu at Department of Astronomy, University of Florida, Florida, USA, for his helpful discussion.

References

[1] Bohren C F and Huffman D R 1983 *Absorption and Scattering of Light by Small Particles* (New York: Wiley) p. 100

[2] John H B and Yuen T L 1971 *IEEE Trans. Antennas Propag.* **19** 378

[3] Mackowski D W 1991 *Proc. R. Soc. London* Ser. A **433** 599

[4] Xu Y L 1995 *Appl. Opt.* **34** 4573

[5] Xu Y L 1996 *J. Comput. Phys.* **137** 285

[6] Xu Y L 1997 *Appl. Opt.* **36** 9496

[7] Xu Y L and Bo A S G 2001 *Journal of Quantitative Spectroscopy & Radiative Transfer* **70** 395

[8] Xu Y L 2003 *J. Opt. Soc. Am.* A **20** 2093

[9] Fuller K A and Kattawar G W 1988 *Opt. Lett.* **13** 1063

[10] Stein S 1961 *Q. Appl. Math.* **19** 15

[11] Wang Y M and Chew W C 1983 *IEEE Trans. Antennas Propag.* **41** 1633

[12] Auger J C, Brian S and Vincent M 2005 *J. Opt. Soc. Am.* A **22** 2700

[13] Bruce T D and Flatau P J 1994 *J. Opt. Soc. Am.* A **11** 1491

[14] Lei C X, Zhang H F and Liu H F 2009 *Acta Phys. Sin.* **58** 7168 (in Chinese)

[15] Barton J P, Alexander D R and Schaub S A 1988 *J. Appl. Phys.* **64** 1632

[16] Gerard G, Grehan G and Bruno M 1988 *Appl. Opt.* **27** 4784

[17] Davis L W 1979 *Phys. Rev.* A **19** 1177

[18] Gerard G, Bruno M and Grehan G 1988 *J. Opt. Soc. Am.* A **5** 1427

[19] Doicu A and Wriedt T 1997 *Appl. Opt.* **36** 2971

[20] Wu Z S, Guo L X, Ren K F, Gouesbet G and Gréhan G 1997 *Appl. Opt.* **36** 5188

[21] Khaled E E M, Hil S C and Barber P W 1993 *IEEE Trans. Antennas Propag.* **41** 295

[22] Barton J P 1995 *Appl. Opt.* **34** 5542

[23] Wu Z S, Yuan Q K, PengY and Li Z J 2009 *J. Opt. Soc. Am.* A **26** 1779

[24] Barton J P, Ma W, Schaub S A and Alexander D R 1991 *Appl. Opt.* **30** 4706

[25] Bai L, Wu Z S, Cheng H and Guo L X 2005 *Acta Phys. Sin.* **54** 2025 (in Chinese)

[26] Edmonds A R 1957 *Angular Momentum in Quantum Mechanics* (Princeton: Princeton University Press)

[27] Zhang H Y and Han Y P 2008 *J. Opt. Soc. Am.* B **25** 255

[28] Tsinopoulos S V, Euripides J S and Demosthenes P 2002 *Appl. Opt.* **41** 1408